Supplemental Material

Myeloid-Specific Deletion of Epsins 1 and 2 Reduces Atherosclerosis by Preventing LRP-1 Downregulation

Authors: Megan L. Brophy, PhD[1,2]; Yunzhou Dong, PhD[1]; Huan Tao, MD, PhD[3]; Patricia G. Yancey, PhD[3]; Kai Song, PhD[1]; Kun Zhang, MD[1,4]; Aiyun Wen, PhD[1]; Hao Wu, PhD[1]; Yang Lee, PhD[1]; Marina V. Malovichko, PhD[5]; Israel D. Sithu, PhD[5]; Scott Wong[1]; Lili Yu[1]; Olivier Kocher, MD, PhD[6]; Joyce Bischoff, PhD[1]; Sanjay Srivastava, PhD[5]; MacRae F. Linton, MD[3]; Klaus Ley, MD[7]; Hong Chen, PhD[1*]

Affiliations:

[1]Vascular Biology Program and Department of Surgery, Boston Children's Hospital and Department of Surgery, Harvard Medical School, Boston, MA, USA

[2]Department of Biochemistry and Molecular Biology, University of Oklahoma Health Sciences Center, Oklahoma City, OK, USA

[3]Atherosclerosis Research Unit, Cardiovascular Medicine, Department of Medicine, Vanderbilt University Medical Center, Nashville, TN, USA

[4]Department of Cardiology, Sun Yat-sen Memorial Hospital of Sun Yat-sen University, Guangzhou, China

[5]Department of Medicine, Division of Cardiovascular Medicine, University of Louisville, Louisville, KY, USA

[6]Department of Pathology and Center for Vascular Biology Research, Beth Israel Medical Deaconess Medical Center, Harvard Medical School, Boston, MA, USA

[7]Division of Inflammation Biology, La Jolla Institute for Allergy and Immunology, La Jolla, CA, USA

Short Title: Myeloid Epsins in Atherosclerosis

***Correspondence:**
Hong Chen, Ph.D.
Harvard Medical School,
Boston Children's Hospital
Karp Family Research Laboratory #12.214
300 Longwood Ave, Boston, MA 02115, USA
E-mail: hong.chen@childrens.harvard.edu
Telephone: 617-919-6304
Fax: 617-730-0232

Online-Only Supplement of Materials and Methods:

Human samples. Diseased aortic arch samples (n=3) from human patients of 16 to 80 years of age containing fatty streaks and normal human patient aortic arch samples (n=3) were obtained from Maine Medical Center Biobank. Paraffin sections were de-paraffinized and processed for antigen retrieval with 10mM Sodium Citrate, pH 6.0, with 0.5% Tween 20 at 90°C for 10 minutes. Slides were then processed for immunofluorescent staining according to standard protocol described below.

Animal model. *ApoE*$^{-/-}$ mice (stock #008525), *LysM-Cre* deleter mice (stock #004781), and *LRP-1*$^{fl/fl}$ mice (stock #012604) were purchased from Jackson Laboratory. We reported a strategy to generate an epsin 1 tissue-specific and epsin 2 global knockout mouse model[1,2]. We used a similar strategy to create a myeloid-specific knockout of espin 1 and a global knockout of epsin2 mouse model. *Epn1*$^{fl/fl}$ mice were mated with *Epn2*$^{-/-}$ mice to generate *epsin1*$^{fl/fl}$; *epsin2*$^{-/-}$ mice. Myeloid-specific double knockout mice (LysM-DKO) were obtained by crossing the *epsin1*$^{fl/fl}$; *epsin2*$^{-/-}$ with LysM-cre$^{+/-}$ mice, which express Cre recombinase specifically in myeloid cells. These mice were then backcrossed onto the C57BL/6 background (Jackson Laboratory stock #00664). The *ApoE*$^{-/-}$;*Epn1*$^{fl/fl}$;*Epn2*$^{-/-}$;LysM-cre$^{+/-}$ mice (ApoE$^{-/-}$/LysM-DKO) were obtained by crossing the LysM-DKO mice with the *ApoE*$^{-/-}$ mice. The *ApoE*$^{-/-}$;*Epn1*$^{fl/fl}$;Ep*n2*$^{-/-}$;*LRP1*$^{fl/+}$;LysM-cre$^{+/-}$ mice (ApoE$^{-/-}$/LysM-DKO-LRP1$^{fl/+}$) were obtained by crossing the *LRP-1*$^{fl/fl}$ mice with the ApoE$^{-/-}$/LysM-DKO mice and backcrossing to C57BL/6 background. To induce atherosclerosis, mice were fed Western diet (WD) (Protein 17% kcal, Fat 40% kcal, Carbohydrate 43% kcal; D12079B, Research diets, New Brunswick, USA) beginning at 6 to 8 weeks of age for 6 to 25 weeks at which point mice were sacrificed and heart, aorta, peritoneal macrophages (Mϕs), and bone marrow were harvested. The ApoE$^{-/-}$ control mice cohort consist of both *ApoE*$^{-/-}$;*Epn1*$^{+/+}$;*Epn2*$^{+/+}$ mice with a single copy of LysM-cre, and *ApoE*$^{-/-}$;*Epn1*$^{fl/fl}$;*Epn2*$^{-/-}$ littermate controls lacking the single copy of LysM-cre, in addition to *ApoE*$^{-/-}$;*Epn1*$^{+/+}$;*Epn2*$^{+/+}$ all of which exhibit no difference in phenotype. Both male and female mice were used throughout this study in separate groups. 10-15 animals were analyzed per time point. This number of mice was estimated by power analysis to be necessary to detect at the 0.05 significance level with a power of 0.80-0.90 and an effect size of 1.55-1.65 SD units with a 2 sample t-test. For studies including PCSK9 virus, LysM-DKO mice and WT mice (including WT, *Epn1*$^{fl/fl}$;*Epn2*$^{-/-}$;*LysM-cre*$^{-/-}$, and *epsin1*$^{+/+}$;*epsin2*$^{+/+}$;*LysM-cre*$^{+/-}$) at 6 to 8 weeks of age were intravenously injected with $2x10^{11}$ genomes of PCSK9 adeno-associated virus (rAAV8-D377Y-mPCSK9 obtained from Boston Children's Hospital Viral Core Facility) followed by 12-22 weeks of WD feeding[3]. Both male and female mice were used for PCSK9-AAV8 injections. Randomization and blinding were adopted for animal studies and sick animals or animals that died prior to a time point were not included in the final analysis. Damaged tissues were not included in the final analysis.

Antibodies and reagents. Unless specified otherwise, common laboratory chemicals and reagents were from either Sigma-Aldrich or Fisher Scientific. Media and additives for cell culture were from Gibco. M-CSF (cyt-439-b) was from Prospec. Lipofectamine 2000 and LTX transfection reagents (11668027, A12621), Image-iT^{TM} signal enhancer (136933), Bodipy^{TM} 493/503 (D3922), CMTPX red cell tracer (C34552), CFDA SE green cell tracer (V12883), and Alexa Fluor conjugated secondary antibodies goat anti-rabbit 647 (A-21244), goat anti-rat 647 (A-21247), donkey anti-mouse 594 (A-21203), donkey anti-rabbit 594 (A-21207), donkey anti-rat 594 (A21209), donkey anti-rat 488 (A-21208), donkey anti-mouse 488 (A-21202), and donkey anti-rabbit 488 (A-21206) were from Invitrogen. The reagents and materials for RNA isolation include Qiagen RNeasy Mini Kit (Qiagen 74106) and Trizol (Ambion 15596026). Reagents for qRT-PCR include the following: RNase-free DNAse 1 (NEB M0303S), SuperScript III First-Strand Synthesis SuperMix (ThermoFisher Scientific 18080400), and SYPR Green PCR Master Mix reagent (GeneCopoeia QP001-01). Aqueous Mounting Medium (CTS011) used in

immunofluorescent staining was from R and D Systems. Oil Red O (0684) was from Amresco, Hematoxylin (H3404) used in conjunction with Oil Red O and VectaMount™ Aqueous Mounting Medium (H-5501) were from Vector. Hematoxylin (GHS3128), Eosin (HT1103128), DAPI (D9542), anti-FLAG M2 affinity Gel (A2220), and Red Blood Cell Lysing Buffer Hybri-Max (R7757) were from Sigma-Aldrich. G sepharose beads (101242), UltraComp eBeads™ compensation beads (01-2222-42), ArC™ Amine Reactive Compensation Bead Kit (A10346), EZ-Link Sulfto-NHS-LC-Biotin (21335), EZ-Link Sulfo-NHS-SS-Biotin (21331), Neutravidin Beads (29200), and Permount Mounting Medium (SP15-500) were from ThermoFisher Scientific. Cholesterol Assay Kit for HDL and LDL/VLDL (ab65390), Triglyceride Assay Kit (ab65336), and Glucose Assay Kit (ab65333) were from Abcam. EDTA tubes Microvette® K3 EDTA tubes (20.1278.100) were from Sarstedt. cOmplete Mini EDTA-free protease inhibitor cocktail (11836170001) was from Roche. FcR Blocking Reagent (101320) was from Miltenyi Biotec. The QuikChange II Site-Directed Mutagenesis Kit was from Agilent Technologies (200524). Oxidized LDL was from Bio-Rad (5685-3557) or made according to previously published protocols[4]. Polyclonal rabbit antibodies for epsin 1 (1:2000 Western blotting dilution; 1:200 immunofluorescent dilution) and epsin 2 (1:2000 Western blotting dilution; 1:200 immunofluorescent dilution) were obtained as described[5-7]. Anti-epsin 1 (SC-8673; 1:200 immunoprecipitation dilution), -LRP-1 (SC-16168; 1:20 Western blotting dilution), -LRP-1 (SC-25469; 1:200 Western blotting dilution; 1:200 immunoprecipitation dilution), -F4/80 (SC-59171; 1:30 immunofluorescent dilution), -CD68 (SC-9139; 1:20 immunofluorescent dilution), and -epsin 1 (SC-55556; 1:50 immunofluorescent dilution) were obtained from Santa Cruz. Anti-LRP-1 (ab92544; 1:5000 Western blotting dilution) was obtained from Abcam. Anti-LDLR (AF2255; 1:1000 Western blotting dilution), -CD36 (MAB2519; 1:500 Western blotting dilution), and fluorochrome conjugated anti-CCR2 (FAB5538P) were obtained from R and D Systems. Anti-ABCA1 (NB400-105; 1:500 Western blotting dilution), and -ABCG1 (NB400-132; 1:400 Western blotting dilution) were obtained from Novus Biologicals. Anti-HA antibody (901502; 1:2000 Western blotting dilution; 1:200 immunoprecipitation dilution) was from Covance. Anti-Flag antibody (F3165; 1:2000 Western blotting dilution), anti-FLAG antibody (F1804, 1:200 immunofluorescent dilution), and anti-actin α Smooth Muscle (C6198; 1:50 immunofluorescent dilution) were from Sigma-Aldrich. Anti-ubiquitin (AUB01; 1:500 Western blotting dilution) was from Cytoskeleton Inc. Anti-α-Tubulin (12G10; 1:1000 Western blotting dilution) was from Developmental Studies Hybridoma Bank. Fluorochrome conjugated anti-CD45 was from BD Biosciences (30-F11). Fluorochrome conjugated anti-F4/80 (123133), -CD11b (101215), -Ly6G (127623), -CD19 (115507), -TCRβ (109223), -Ly6C (128014), -CX3CR1 (149035) were from Biolegend. Collagenase I (17100-017) was from Gibco and collagenase XI (C7657) and hyaluronidase I-S (H3506) were from Sigma-Aldrich.

Atherosclerosis analysis. Mice were sacrificed with isoflurane. Blood was removed from the right atrium and vascular perfusion performed with cold PBS. Hearts isolated from mice were fixed in 4% PFA and cryopreserved in OCT and immediately frozen or fixed in 10% Formalin and processed for paraffin embedding by the Rodent Histopathology Core at Harvard Medical School. The aortic sinus in the heart was sectioned from cryoblocks or paraffin blocks at 10 microns. Lesion size of aortic root was quantified to confirm consistency of lesion size measurements determined by the *en face* approach by quantifying sections at intervals of 80 microns using National Institutes of Health (NIH) ImageJ software[8-10] (approximately 9-12 sections analyzed per aortic root). This software was used to manually trace the internal elastic lamina and luminal boundary of the lesion and provide the percent of lesion area of aortic root. By analyzing several sections, a topographic profile of the lesion throughout the aorta is created. Cryosections were stained with Oil Red O or immunofluorescent staining performed as described below with anti-CD68 or anti-F4/80 antibodies. Oil Red O imaging was performed with a Zeiss Axio Scope.A1, AxioCam ICc5, and ZEN-Lite 2012 software. Immunofluorescent

imaging performed as described below. For *en face* aorta analysis, whole aortas were isolated after PBS perfusion, split, pinned, and fixed in 4% PFA followed by Oil Red O staining. Imaging of aortas was performed using a Nikon SMZ1500 stereomicroscope, SPOT Insight 2Mp Firewire digital camera, and SPOT Software 5.1. Quantification of lesions was performed by manually tracing the aorta and lesion areas with NIH ImageJ software[8-10]. Studies analyzing mouse phenotype including Oil Red O, H and E, and IF staining, were performed with blinding in which each animal was assigned a number and data was collected based on the assigned number with genotype and experimental condition unknown to the data collector.

Oil Red O staining. For cryosections, slides were washed 3 times with PBS for 5 minutes each, and incubated in 100% propylene glycol for 2-5 minutes followed by incubation in pre-warmed (60°C) 0.5% Oil Red O solution for 10 minutes at 60°C. Slides were then incubated in 85% propylene glycol for 2-5 minutes followed by 3 washes with diH_2O, incubation with hematoxylin (Vector; diluted 1:5 in dH_2O) for 30 seconds, 3 washes with diH_2O, and mounting of coverslips with VectaMount[11]. For coverslips with primary macrophages, coverslips were washed 3 times with PBS for 5 minutes each and incubated in pre-warmed (65°C) 0.5% Oil Red O solution for 10 minutes at 65°C. Slides were then washed 3 times for 5 minutes each in PBS, incubated with hematoxylin (Vector; diluted 1:2 in dH_2O) for 30 seconds, washed with PBS 3 times, and mounted of coverslips with Aqueous Mounting Media onto slides[11]. Imaging was performed with a Zeiss Axio Scope.A1, AxioCam ICc5, and ZEN-Lite 2012 software. Quantification of lesion was performed as described above. Quantification of foam cells was performed as described below.

Necrotic area of lesion analysis. For H and E staining, mouse aortic root paraffin sections were deparaffinized in 100% Xylenes, incubated in 50:50 Xylenes:100% ethanol, and hydrated in 100% ethanol, 95% ethanol, and H_2O successively. Slides were stained with hematoxylin (Sigma-Aldrich) followed by washes in tap water, acid alcohol, tap water, ammonia water, and tap water. Slides were then stained with eosin followed by washes in tap water, dehydration in 95% and 100% ethanol, incubation in 50:50 Xylenes:100% ethanol, incubation in 100% Xylenes, and mounting of coverslips with Permount following standard protocols[12]. Imaging was performed with a Zeiss Axio Scope.A1, AxioCam ICc5, and ZEN-Lite 2012 software. Lesion area was traced as described above using NIH ImageJ software in addition to necrotic or acellular regions within the lesion to determine the percentage of necrotic area of the lesion[12].

Analysis of plasma glucose, triglyceride, and cholesterol levels. Blood was removed from the right atrium of the mouse heart after sacrifice with isoflurane. Blood was allowed to clot for 30 minutes at room temperature followed by centrifugation at 10000xg at 4°C for 20 minutes. Serum was transferred to a new tube and stored at -20°C[13]. Serum cholesterol and lipid levels were determined using the Cholesterol Assay Kit for HDL and LDL/VLDL and Triglyceride Assay Kit from Abcam. Fasting blood glucose levels were measured from mice fasted for 4 hours with access to water. Serum glucose levels were measures using the Glucose Assay Kit from Abcam.

Analysis of plasma lipoproteins in PCSK9 mice. Blood was removed from the right atrium of the mouse heart after sacrifice with isoflurane. Blood was allowed to clot for 30 minutes at room temperature followed by centrifugation at 10000xg at 4°C for 20 minutes. Serum was transferred to a new tube and stored at -20°C[13]. Levels of cholesterol in the plasma were measured as previously described[14-16]. Cholesterol distribution in the lipoproteins was assessed by size exclusion chromatography on FPLC as previously described[15,16].

Peripheral blood counts. Blood was collected from the right atrium of the mouse heart after sacrifice with isoflurane and collected into EDTA tubes. Peripheral blood counts of myeloid cells

were measured with a Hemavet 950 veterinary hematology analyzer (Drew Scientific, Inc.) from whole blood[17-19].

Immunofluorescent staining. Human aorta samples and mouse aortic root paraffin sections were deparaffinized and hydrated followed by antigen retrieval with 10mM Sodium Citrate, pH 6.0, with 0.5% Tween 20 at 90°C for 10 minutes prior to blocking and staining. Mouse aortic root cryosections were blocked in PBS solution containing 3% donkey and/or goat serum, 3% BSA, and 0.3% Triton X-100. Sections were then treated with Image-iT^{TM} FX signal enhancer and incubated with primary antibody overnight at 4°C, followed by incubation with the respective secondary antibodies conjugated to fluorescent labels (Alexa Flour 594, 488, or 647; 1:200 to 1:500) for 1 hour at room temperature. Bodipy^{TM} 493/503 staining of tissue sections was performed following secondary antibody incubation[20,21]. Slides were washed in PBS, stained with DAPI, mounted, and immunofluorescent images were obtained using an Olympus IX81 Spinning Disc Confocal Microscope with an Olympus plan Apo Chromat 4x and 10x objective and Hamamatsu Orca-R2 Monochrome Digital Camera C1D600 equipped with Slidebook 5 software. Tissues stained with omission of primary antibody were captured using the same settings and were used as negative controls. Mean fluorescence intensity of antibody staining within atheroma region was determined via ImageJ software with n=3 or more[2,22-24].

Primary mouse macrophage isolation and culture. For elicited peritoneal macrophages (Mϕs), mice were injected with 1mL of 3% thioglycolate. At day 3 post-injection, mice were sacrificed and 7mL of sterile 1X PBS were injected into the peritoneal cavity. The abdomen was massaged for approximately 5 minutes and then PBS was extracted from the peritoneal cavity. Cells were spun down (1000xg, 5 minutes), washed with PBS, and plated in RPMI (supplemented with 10% FBS, 1% PennStrep). After 24 hours, cells were washed with PBS to remove non-Mϕ cells[25]. Thioglycolate injection was not performed for non-elicited peritoneal Mϕs. For bone marrow-derived Mϕs, mice were sacrificed and both femurs and tibias were dissected and flushed with sterile 1X PBS, which was passed through a 100μM cell strainer and collected. The cells were spun down (1000xg, 5 minutes), washed with 1X PBS, and plated in RPMI (supplemented with 10% FBS, 1% PennStrep) with M-CSF (10ng/mL). Cells were allowed to differentiate into Mϕs for 5 days after which cells were harvested or media was changed daily. All primary cells were cultured at 37°C with 5% CO_2[25]. Both bone marrow-derived and elicited peritoneal primary Mϕs were used to confirm knock out of epsin 1 and epsin 2. Elicited peritoneal Mϕs were primarily used for Western blots and immunoprecipitations due to higher yields.

Cell culture. The HEK 293T cell line (ATCC no. CRL-11268) and RAW264.7 cell line (mouse Mϕ cells transformed with murine leukemia virus, ATCC no. TIB-71) were cultured in DMEM or RPMI, respectively, supplemented with 10% FBS and 1% PennStrep at 37°C with 5% CO_2. WT and DKO mouse embryonic fibroblasts were isolated and cultured as previously described[1].

Plasmids and transfections. Epsin 1, Epsin1ΔUIM, truncation constructs, and single domain constructs were described previously[26]. HA-tagged mLRP4T100 mutations (HA tag to FLAG tag and lysine residues to arginine residues) were made using the QuikChange Site-Directed Mutagenesis Kit as per the manufacturer's instruction. Mutagenesis primers are listed in **Online Table I**. HEK 293T cells were transfected using Lipofectamine 2000 as instructed by the manufacturer[2,22-24,27,28].

RNA isolation and quantitative real-time PCR. Total RNA was extracted from primary Mϕs with Qiagen RNeasy Mini Kit or Trizol per manufacturers' instructions. One microgram of total RNA was treated with 1 U RNase-free DNase 1 to eliminate genomic DNA. The first-strand cDNA was synthesized using the SuperScript III First-Strand Synthesis SuperMix. 2 μl of the product was subjected to qRT-PCR in a 7300 Real-Time PCR System or StepOnePlus Real-

Time PCR System (Applied Biosystems) using SYBR Green PCR Master Mix reagent as the detector. PCR amplification was performed in triplicate on 96-well optical reaction plates and replicated in at least three independent experiments. The ΔΔCt method was used to analyze qPCR data. The Ct of β-actin cDNA was used to normalize all samples[29,30]. Primers are listed in **Online Table II**.

Immunoprecipitation and Western blotting. For total protein levels, primary Mϕs were washed with ice cold PBS, lysed in 2X Laemmli buffer and processed for Western blotting. For immunoprecipitations, cells were washed with ice cold PBS and lysed with lysis buffer (1% Triton X-100, 5mM Na_3VO_4, 10mM N-ethylmaleimide, and protease inhibitor cocktail). Cell Lysates were centrifuged at 10000xg for 10 minutes at 4°C to separate cellular debris. Cell lysates were pre-cleared with appropriate species of IgG and protein G Sepharose beads for 1 h at 4°C with rotation followed by incubation with G Sepharose beads and indicated antibodies or anti-FLAG M2 affinity Gel for 4 to 12 hours at 4°C with rotation. For negative controls, equal concentration of mouse IgG was added instead of specific antibodies. Precipitated proteins were eluted from beads using 4X Laemmli buffer diluted 1:3 in lysis buffer followed by Western blotting. Proteins were resolved by SDS-PAGE (7.5% or 10% acrylamide) followed by electroblotting to polyvinylidene difluoride membrane and blocking with 5% milk (weight per volume) according to standard procedures. Primary antibodies were incubated at 4°C overnight followed by incubation with respective horseradish peroxidase-conjugated secondary antibodies (1:1000 or 1:2000) at room temperature for 1 hour. The immunoreactive proteins were detected by enhanced chemiluminescence with autoradiography. Western blotting densitometry quantifications were performed with NIH ImageJ software with n=3 or more. Total protein levels were normalized to Tubulin levels. Co-immunoprecipitated protein levels were normalized to pull down of IgG, FLAG-tagged protein, LRP-1, or Epsin 1. For IPs in RAW cells involving oxLDL treatment, cells were treated for 4 hours with 1 μM MG132 in serum-free media, followed by stimulation with oxLDL (200μg/mL) for 30 minutes at 37°C and prepared for immunoprecipitation. 100-200μg/mL was used as it falls well within the range of oxLDL levels found within the vessel wall[31,32]. For experiments involving transfection of LRP-1 constructs and epsin 1 constructs, HEK 293T cells were treated with oxLDL (100-200μg/mL) 16 hours post-transfection for 30 minutes at 37°C and prepared for immunoprecipitation[2,22].

Foam cell formation. Elicited peritoneal or bone marrow-derived Mϕs were isolated and plated on 12mm glass coverslips with 0.2% gelatin and allowed to differentiate with M-CSF in the case of bone marrow-derived Mϕs. Cells were cultured in RPMI supplemented with 10% lipid-depleted serum and 1% PennStrep for 24-48 hours and then treated with 10-100 μg/mL oxLDL for 24 hours. Cells were fixed in 4% PFA for 10 minutes at room temperature and washed with PBS. For Oil Red O staining, coverslips were stained with Oil Red O, washed with PBS, counterstained with hematoxylin, washed with PBS, and then mounted on slides. For Bodipy staining, coverslips were immunofluorescently stained with F4/80 overnight and stained with the appropriate secondary antibody followed by staining with Bodipy™ 493/503 for 1 hour at 37°C, counterstaining with DAPI, and mounting on slides. Negative controls were not treated with oxLDL[33]. Foam cells were determined as the number of lipid positive cells (Oil Red O positive or Bodipy and F4/80 positive) as a percentage of total cells. At least 5 fields per cover slip and 5 mice per genotype were used for quantification.

Efferocytosis assay. *In vitro*: primary elicited peritoneal Mϕs from female mice were cultured and labeled with CMTPX red cell tracer. Cells were washed with PBS and serum starved overnight. Apoptosis was induced in WT thymocytes labeled with CFDA SE green cell tracer via 600 rad irradiation. The apoptotic cells were added to primary Mϕ cultures for 2 hours. Efferocytosis was visualized using fluorescence microscopy. *In vivo*: WT thymocytes were labeled with CFDA-SE and induced to undergo apoptosis with 600 rad irradiation. $1x10^9$

apoptotic labeled thymocytes were injected into WT and LysM-DKO female mice, which had been injected with thioglycolate 2 days prior. Two hours post injection with apoptotic cells, peritoneal Mϕs were isolated, plated, and labeled with CMTPX red cell tracer. Primary Mϕs were scraped and efferocytosis analyzed via flow cytometry. Percent efferocytosis was quantified as the number of macrophages with engulfed apoptotic cells as a percentage of the total number of macrophages[12,34].

Flow cytometry analysis. *Flow cytometry of aortas*: Mice on Western diet were sacrificed with isoflurane. Perfusion was performed with sterile 1X PBS. Aortas were dissected, homogenized, and placed in an enzyme solution containing collagenase type I (1.4mg/mL), hyaluronidase type I-S (60U/mL), collagenase type XI (125U/mL), and DNAse I (1U/mL) in PBS with 10mM Hepes (pH 8.4) for 45-55 minutes at 37°C shaking. Enzyme solution with aortic derived cells were put through 100μM strainers and rinsed with 20mL 1X PBS. Cells were centrifuged (300xg, 8 minutes), resuspended in RPMI medium (10% FBS, 5% PennStrep, 1X L-Glutamine, 1X Sodium Pyruvate, 25mM HEPES, 1X MEM NEAA), and incubated at 37°C for 30 minutes. Cells were centrifuged and resuspended in 1X PBS followed by Zombie Red staining according to manufacturer's protocol. Cells were washed with FACS Buffer (1X PBS, 2% FBS, 2mM EDTA) and resuspended in FACS buffer containing the following: FcR Blocking Reagent, and fluorochrome conjugated anti-CD45, -CD11b, -F4/80, -TCRβ, -CD19, -Ly6C, and -Ly6G. Cells were washed with FACS buffer, fixed with 2% PFA, and resuspended in FACS buffer for analysis. Fluorescence minus one controls were prepared using cells isolated from mouse spleens, which were treated the same as mouse aortas. No color controls were prepared using cells isolated from mouse spleen using the same methods for aortas. Single color controls were prepared using UltraComp eBeads™ Compensation Beads and ArC™ Amine Reactive Compensation Bead Kit. Expression of immune and inflammatory cell markers was analyzed using a BD LSRII Flow Cytometry with DIVA software version 8 or FlowJo version 10 software. Gating strategies were performed as described in **Online Figure V**[35-37]. To analyze pro-inflammatory and anti-inflammatory populations of monocytes, aortas and cells were processed as above but stained with Zobmie Red and fluorochrome conjugated anti-CD45, -CD11b, -Ly6G, -Ly6C, -CX3CR1, and -CCR2[38-40]. *Flow cytometry of peripheral blood mononuclear cells*: 3 drops of blood from the lateral saphenous vein were collected into 1.5mL Eppendorf tubes containing 200μL of PBS (without Ca^{2+} and Mg^{2+}) with 10mM EDTA on ice[41]. 500μL of cold Red Blood Cell Lysing Buffer (Sigma-Aldrich) was added followed by vortexing and incubation at room temperature according to manufacturer protocols. After completion of lysis, 500μL of cold FACS buffer was added and cells were centrifuged (300xg, 8 minutes). Cells were resuspended in 1mL of 1X PBS followed by Zombie Red staining, antibody staining, and fixation as described above. Fluorescence minus one and no color controls were prepared using PBMCs from WT mice. Expression of immune and inflammatory cell markers was analyzed as described above[42]. *Flow cytometry of bone marrow cells*: Bone marrow was isolated from both femurs and tibias of each mouse as described above and spun down (1000xg, 5 minutes). Red blood cell lysis was achieved by resuspending the cells in 20mL of 0.2% NaCl for approximately 20 seconds followed by the addition of 20mL of 1.6% NaCl. Cells were spun down, and washed with FACS buffer. Cells were centrifuged and resuspended in 1X PBS followed by Zombie Red staining, antibody staining, and fixation as described above. Fluorescence minus one and no color controls were prepared using bone marrow cells from WT mice. Expression of immune and inflammatory cell markers was analyzed as described above[42,43].

Cell surface biotinylation. Primary elicited peritoneal Mϕs in culture were washed with cold PBS and treated with 2mM EZ-Link Sulfo-NHS-LC-Biotin on ice for 30 minutes followed by 3 washes for 5 minutes each of 50mM Glycine and then 3 washes for 5 minutes each of cold PBS. Cells were lysed and processed for streptavidin bead pull down: cells were lysed with lysis

buffer, cell lysates were incubated with neutravidin beads for at least 12 hours at 4°C with rotation, and proteins were eluted from beads using 4X Laemmli buffer diluted 1:3 in lysis buffer. Cell surface biotinylated proteins were analyzed by Western blotting and densitometry and quantified by NIH Image J software with n=5[2,23]. Surface protein levels were normalized to surface levels of LDLR.

Cell surface biotinylation with internalization. Primary elicited peritoneal Mϕs (5 60mm dishes per genotype per experiment) in culture were washed with cold PBS and treated with 2mM EZ-Link Sulfo-NHS-SS-Biotin on ice for 30 minutes followed by 3 washes for 5 minutes each of 50mM Glycine on ice and then 3 washes for 5 minutes each of cold PBS on ice. 3 plates of cells of each genotype were treated with 10μg/mL of oxLDL in serum-free RPMI for 5, 10, and 15 minutes at 37°C. Cells were washed 3 times with cold PBS for 5 minutes on ice. Plates treated with oxLDL and 1 additional plate were treated 2 times with cold cleavage buffer (23mM NaH_2PO_4, 27mM Na_2HPO_4, 75mM NaCl, 1% BSA, 10% EDTA, 50mM DTT in dH_2O, pH 8.0) on ice for 15 minutes each followed by 3 washes with cold PBS on ice. Cells were lysed and processed for streptavidin bead pull down as described above[2,23]. Cell surface biotinylated proteins and internalized biotinylated proteins were analyzed by Western blotting and densitometry and quantified by NIH Image J software with n=5. Percent internalized protein was determined as follows: (density of internalized protein band – density of cleavage control lane)/density of surface protein band x 100.

Antibody feeding with internalization. WT and DKO mouse embryonic fibroblasts (MEFs) were plated onto 12mm coverslips in 24 well plates and transfected with FLAG-tagged mLRP4T100 plasmids with Lipofectamine LTX as instructed by the manufacturer[44]. Approximately 18 hours post-transfection, coverslips were washed 2 times with cold PBS on ice for 5 minutes each followed by incubation with anti-FLAG antibodies (1:200) in ice cold PBS on ice for 30 minutes. Coverslips were washed with ice cold PBS. For cell surface levels of transfected LRP-1, coverslips were fixed with 4% PFA. For internalization, coverslips were treated with 10μg/mL of oxLDL in serum-free RPMI at 37°C for 5, 10, and 15 minutes followed by 2 washes with cold PBS and 2 washes with ice cold antibody stripping buffer (0.5M NaCl and 0.2M acetic acid in PBS) for 2 minutes each on ice[45]. Coverslips were washed with cold PBS on ice and fixed with 4% PFA. After fixation, coverslips were permeabilized and blocked in PBS containing 3% donkey serum, 3% BSA, and 0.3% Triton X-100 followed by incubation with donkey anti-mouse 488 secondary antibodies (1:400) for 1 hour. Coverslips were washed with PBS, incubated with DAPI (1:1000) for 5 minutes, washed with PBS, and mounted on slides. Immunofluorescent images were obtained using an Olympus IX81 Spinning Disc Confocal Microscope with an Olympus plan Apo Chromat 60x objective and Hamamatsu Orca-R2 Monochrome Digital Camera C1D600 equipped with Slidebook 5 software. Coverslips stained with omission of plasmid transfection were captured using the same settings and were used as negative controls. To quantify internalization of LRP-1, corrected total cell fluorescence of 15-25 cells per condition was determined using NIH Image J software. The percentage of internalized was determined by subtracting the average background intensity from the intensity of internalized receptors and dividing by the average of surface intensity[45].

Study approval. All animal studies were performed in compliance with institutional guidelines and were approved by Institutional Animal Care and Use Committee (IACUC), Oklahoma Medical Research Foundation, Oklahoma City, OK or IACUC, Boston Children's Hospital, Boston, MA.

Statistical analysis. Data are shown as mean $\pm$ standard error (SE). Normality was determined using D'Agostino-Pearson normality testing for experiments with $n \geq 8$ and Kolmogorov-Smirnov normality testing for experiments with $n<8$. Data for experiments with two groups were analyzed

by the unpaired student's t test or Mann-Whitney U test where appropriate. Data from experiments with multiple groups were analyzed with ANOVA with Bonferroni test or Dunn's multiple comparison test where appropriate. P value < 0.05 was considered significant. Statistical analysis was performed using GraphPad Prism version 7.03 for Windows.

Online Supplemental Figures and Legends:

Online Figure I. Epsin 1 expression is increased in macrophages in human atherosclerotic patient lesion samples. Normal human aortic arch sample (n=3) and atherosclerotic (AS) patient aortic arch samples (n=3) ages 16-80 years with lesion were stained for epsin 1 (green) and CD68 (Mϕ, red). Scale bar=200μM. *Normal aorta group *vs.* AS patient aorta group, P<0.01.

Online Figure II. Myeloid-specific deletion of epsins deletes epsins from primary macrophages. A. *LysM-Cre$^{+/-}$* mice were crossed with *Epsin1$^{fl/fl}$;Epsin2$^{-/-}$ mice to generate a myeloid-specific deletion of epsins mouse (LysM-Cre$^{+/-}$;Espin1$^{fl/fl}$;Epsin2$^{-/-}$ or LysM-DKO*). **B.** Bone marrow-derived and elicited peritoneal Mϕs were isolated from WT (n=5) and LysM-DKO (n=5) mice and lysed for Western blot. Total protein levels of epsin 1 and epsin 2 were normalized to Tubulin. *LysM-DKO goup *vs.* WT group, P<0.01.

Online Figure III. Epsins 1 and 2 are absent in macrophage-rich regions of aortic root sections from ApoE$^{-/-}$/LysM-DKO mice fed Western diet (WD). Aortic root sections from ApoE$^{-/-}$ and ApoE$^{-/-}$/LysM-DKO mice fed WD for 20 weeks were stained with anti-epsin 1 (**A**) or –epsin 2 (red) (**B**) and -F4/80 antibodies (green). Scale bar=200μM.

Online Figure IV. Myeloid-specific deletion of epsins does not alter immune and inflammatory cell populations in blood and bone marrow. Cells from blood (**A**) and bone marrow (**B**) from ApoE$^{-/-}$ (n=5) and ApoE$^{-/-}$/LysM-DKO (n=6) mice were isolated, labeled with Zombie Red, CD45 (hematopoietic cells), CD11b, F4/80, CD19, TCRβ, Ly6C, Ly6G, and analyzed via flow cytometry to determine populations of macrophages (F4/80+;CD11b+), monocytes (Ly6C+;Ly6G-), neutrophils (Ly6C+;Ly6G+), T cells (TCRβ+), and B cells (CD19+). No significance (NS), ApoE-/- group *vs.* ApoE-/-/LysM-DKO group.

Online Figure V. Gating strategy for flow cytometric analysis of immune and inflammatory cell population of mouse aortas, PBMCs, and bone marrow. Aortas from ApoE$^{-/-}$ and ApoE$^{-/-}$/LysM-DKO mice fed Western diet were isolated, digested, cells isolated, and labeled with Zombie Red, CD45 (hematopoietic cells), CD11b, F4/80, CD19, TCRβ, Ly6C, and Ly6G. Blood and bone marrow were harvested and labeled as described. **A.** The major leukocyte population was selected in forward versus side scatter scatter plots and single cell determination was performed. Live CD45+ (Zombie Red-) cells were then selected for further analysis. **B.** Subsets of immune and inflammatory cells were gated as shown. Neutrophils are Ly6G+;Ly6C+, monocytes are Ly6+;Ly6G-, B cells are CD19+, T cells are TCRβ+, and macrophages are CD11b+;F4/80+. **C.** Pro- and anti-inflammatory populations of monocytes in mouse aortas were determined by gating for live CD45+ cells and monocytes as described. The monocyte population was further gated to determine CCR2+ (pro-inflammatory monocyte) and CX3CR1+ (anti-inflammatory monocyte) cells.

Online Figure VI. Lipid content within the lesion is reduced in mice with a myeloid-specific deletion of epsins. Aortic root sections from ApoE$^{-/-}$ (n=7) and ApoE$^{-/-}$/LysM-DKO (n=7) mice fed Western diet for 10 weeks were stained with Bodipy (lipids, green), CD68 (macrophage, red), and DAPI (blue). Scale bar =200μM. *ApoE$^{-/-}$ group *vs.* ApoE$^{-/-}$/LysM-DKO group, P<0.01.

Online Figure VII. Myeloid-specific deletion of epsins alters pro- and anti-inflammatory monocyte populations in mouse aortas. Aortas from ApoE$^{-/-}$ (n=3) and ApoE$^{-/-}$/LysM-DKO

(n=3) were isolated, digested, cells isolated, labeled with Zombie Red, CD45 (hematopoietic cells), Ly6C (monocytes), Ly6G (neutrophils defined as Ly6C+;Ly6G+), CCR2 (pro-inflammatory monocytes), and CX3CR1 (anti-inflammatory monocytes), and analyzed via flow cytometry. *****ApoE-/- goup *vs.* ApoE-/-/LysM-DKO group, P<0.05.

Online Figure VIII. Myeloid-specific deletion of epsins in a PCSK9-AAV8 injection model of atherosclerosis ameliorates the development of atherosclerosis and reduces foam cell formation. Both WT (n=14) and LysM-DKO (n=14) mice injected with PCSK9-AAV8 ($2x10^{11}$ genomes) and fed Western diet (WD) for 12-22 weeks were obtained. **A.** Aortic root sections from WT and LysM-DKO mice (fed WD for 12 weeks) were stained with Oil Red O. Scale bar=200μM. **B.** Atherosclerotic lesion area of aortic root from WT and LysM-DKO mice (fed WD for 12 weeks). *WT-PCSK9 group *vs.*LysM-DKO-PSCK9 group, P<0.01.**C.** En face aortas from WT and LysM-DKO mice were stained with Oil Red O (fed WD for 22 weeks). Scale bar=250μM. **D.** Aortic root sections from WT and LysM-DKO mice (fed WD for 22 weeks) were stained with Oil Red O. Scale bar=200μM. **E.** Atherosclerotic lesion area of aortic root from WT and LysM-DKO mice (fed WD for 22 weeks). *WT-PCSK9 group vs.LysM-DKO-PSCK9 group, P<0.01. **F.** Elicited peritoneal macrophages from WT(n=14) and LysM-DKO (n=14) mice injected with PCSK9-AAV8 ($2x10^{11}$ genomes) and fed WD for 12 weeks were treated with oxLDL (25ug/ml, 24 hours) and stained with Oil Red O. Scale bar=20μM. n=14. *WT-PCSK9 group *vs.* LysM-DKO-PCSK9 group, P<0.001.

Online Figure IX. Myeloid-specific deletion of epsins in a PCSK9 model of atherosclerosis does not alter serum cholesterol levels. Lipoprotein profiles from serum of WT and LysM-DKO mice injected with PCSK9-AAV8 ($2x10^{11}$ genomes) and fed Western diet (WD) for 12 weeks were obtained. **A.** Total serum cholesterol levels from WT-PCSK9 (n=8) and LysM-DKO-PCSK9 (n=8) mice fed WD were measured. No significance (NS), WT-PCSK9 group *vs*. LysM-DKO-PCSK9 group. **B.** Representative chromatogram of the separation of lipoproteins on fast protein liquid chromatography (FPLC) on a Superose 6 column equilibrated with PBS. Plasma (containing 200μg cholesterol) was applied to the column and samples were eluted isocratically with PBS. Cholesterol recovered in FPLC eluate (0.5mL fractions) was measured as described. **C.** Distribution of cholesterol in lipoprotein fractions. n=8. No significance (NS), WT-PCSK9 group *vs*. LysM-DKO-PCSK9 group. **D.** Western blot of liver lysates from WT, WT-PCSK9, and LysM-DKO-PSCK9 mice. n=4, respectively. *WT group *vs.* (WT-PCSK9, LysM-DKO-PSCK9) group, P<0.01.

Online Figure X. Myeloid-specific deletion of epsins increases efferocytosis and shifts macrophage phenotype to anti-inflammatory. A. WT CFDA-SE labeled thymocytes (green) were injected into WT, LysM-DKO, $ApoE^{-/-}$, and $ApoE^{-/-}$/LysM-DKO mice 2 hours prior to harvesting elicited peritoneal Mϕs. Harvested cells were labeled with CMTPX (red) and analyzed by flow cytometry for percent efferocytosis. PE positive cells were designated macrophages. GFP positive cells were designated apoptotic cells. Double positive cells were apoptotic cells engulfed by macrophages (efferocytosis). n=5. *LysM-DKO group *vs.* WT group, P<0.05; # ApoE-/-/LysM-DKO *vs.* ApoE-/-, P<0.05. **B.** Bone marrow-derived Mϕs isolated from $ApoE^{-/-}$(n=3) and $ApoE^{-/-}$/LysM-DKO (n=3) mice were treated with TNFα (20ng/mL) followed by RNA isolation, cDNA preparation, and qPCR for indicated genes. *ApoE-/-/LysM-DKO+TNFα group *vs.* ApoE-/- + TNFα group, P<0.05. RNA was isolated from non-elicited peritoneal Mϕs (**C**) and bone marrow-derived Mϕs (**D**) from WT (n=3) and LysM-DKO (n=5) mice, cDNA was made,

and qPCR was performed with the indicated primer pairs. *LysM-DKO group *vs.* WT group, P<0.01.

Online Figure XI. LRP-1 total and surface levels are increased with no change in transcription and decreased internalization in macrophages from myeloid-specific epsins deficient mice. A. Quantification of western blot (WB) for total protein levels in elicited peritoneal Mϕs from WT (n=5) and LysM-DKO (n=5) mice (**Figure 4b**). Total protein levels were normalized to Tubulin. *LysM-DKO group *vs.* WT group, P<0.01. **B.** Quantification of WB for surface protein levels in elicited peritoneal Mϕs from WT (n=3) and LysM-DKO (n=3) mice that were biotinylated and processed for neutravidin beads pull down (**Figure 4c**). Surface protein levels were normalized to LDLR or CD36 surface levels. *LysM-DKO group *vs*. WT group, P<0.01. **C.** RNA was isolated from WT (n=3) and LysM-DKO (n=3) bone marrow-derived Mϕs, cDNA was made, and qPCR was performed using primer pairs for the indicated genes. No significance (NS), LysM-DKO group *vs.* WT group. **D.** Quantification of WB of surface and internalized biotinylated proteins in WT (n=5) and LysM-DKO (n=5) elicited peritoneal macrophages treated with or without oxLDL (10μg/mL) and with or without cleavage buffer to strip the biotin from the surface of cells. Percent internalization was determined by dividing the density of internalized band by the density of surface level band (**Figure 4d**). *LysM-DKO group *vs*. WT group, P<0.01 for LRP-1 internalization. No significance (NS), for LDLR and ABCA1 internalization.

Online Figure XII. Epsins deletion ameliorates LRP-1 internalization in MEFs. A. Quantification for **Figure 4e**. WT and DKO MEFs were transfected with FLAG-tagged LRP1. Cells were labeled with anti-FLAG antibodies. Surface levels of FLAG-LRP1 were determined by staining with 488 conjugated secondary antibodies and DAPI. Antibody stripping control cells were treated with antibody stripping buffer followed by staining with 488 conjugated secondary antibodies and DAPI. Other cells were treated with oxLDL (10μg/mL) for the indicated time points followed by treatment with antibody stripping buffer and staining with 488 conjugated antibodies and DAPI. n=15-25. *DKO group vs. WT group, P<0.01. **B**. Images of antibody stripping control cells taken at 20X. Scale bar=20μm. **D**. Western blot of WT and DKO MEFs transfected with FLAG-tagged LRP1 plasmid.

Online Figure XIII. Macrophage epsin interacts with LRP-1 endogenously but not with CD36, ABCA1, or LDLR. WT elicited peritoneal macrophages were lysed and processed for IP with anti-Epsin 1 antibodies followed by WB. n=3. *LRP-1 Co-IP group v*s.* IgG group, P<0.01.

Online Figure XIV. Mutation of 3 C-terminal lysine residues in LRP-1 reduce ubiquitination of LRP-1. A. Combinations of 3 lysine residues in the cytoplasmic tail of the LRP-1 minireceptor were mutated to arginine via site-directed mutagenesis. **B.** 293T cells were transfected with FLAG tagged LRP-1 constructs: LRP-1 control (mLRP4T100) and mutant constructs. Cells (n=3) were treated with oxLDL (200μg/mL,30min), lysed, and processed for IP with anti-FLAG beads followed by Western blot with indicated antibodies. Ubiquitin co-IP was normalized to FLAG IP. *FLAG-LRP1 + oxLDL group *vs.* FLAG-LRP1-K30/54/83R + oxLDL group, P<0.01.

Online Supplemental Tables:

Online Table I. Primers for mutagenesis of LRP-1 minireceptor.

Target		Primer Sequence
HA tag to FLAG tag	Forward	5'- GTCGCGGCGGCTATCGACGCCGACTACAAGGACGACGATGA CAAGGGATCCCCCTGCAAGGTCAAC-3'
	Reverse	5'- GTTGACCTTGCAGGGGGATCCCTTGTCATCGTCGTCCTTGTA GTCGGCGTCGATAGCCGCCGCGAC-3'
Lysine 30 to Arginine	Forward	5'- GATTGGAAACCCCACCTACAGGATGTACGAAGGCGGAG-3'
	Reverse	5'- CTCCGCCTTCGTACATCCTGTAGGTGGGGTTTCCAATC-3'
Lysine 54 to Arginine	Forward	5'- CTTTGCCCTGGACCCTGACAGGCCCACCAACTTCACCAAC-3'
	Reverse	5'- GTTGGTGAAGTTGGTGGGCCTGTCAGGGTCCAGGGCAAAG-3'
Lysine 83 to Arginine	Forward	5'- GGCCAGCACGGACGAGAGGCGAGAACTCCTGGGCC-3'
	Reverse	5'- GGCCCAGGAGTTCTCGCCTCTCGTCCGTGCTGGCC-3'

Online Table II. Primers for qPCR.

Target		Primer
Arg1	Forward	5’-CAGTGGCTTTAACCTTGGCT-3’
	Reverse	5’-GTCAGTCCCTGGCTTATGGT-3’
β-Actin	Forward	5’-TTACTGCTCTGGCTCCTAGCA-3’
	Reverse	5’-CCACCGATCCACACAGAGTAC-3’
CD11c	Forward	5’-GGTCCTACTGTGCACCACAC-3’
	Reverse	5’-TCTTGCTTTGGACACTCCTG-3’
CD163	Forward	5’-GGGTCATTCAGAGGCACACTG-3’
	Reverse	5’-CTGGCTGTCCTGTCAAGGCT-3’
Epsin 1	Forward	5’-CTACCAACGTCCATTGCGGT-3’
	Reverse	5’-GCAGCGATGAGGTCGACATT-3’
Epsin 2	Forward	5’-TCTATCAGACGGCAGATGAAAAAC-3’
	Reverse	5’-GTCATTGGAGGTGGCCTCC-3’
IL-1β	Forward	5’-GAAGAAGAGCCCATCCTCTG-3’
	Reverse	5’-TCATCTCGGAGCCTGTAGTG-3’
IL-6	Forward	5’-AGTCCGGAGAGGAGACTTCA-3’
	Reverse	5’-TTCCACGATTTCCCAGAG-3’
IL-10	Forward	5’-CCCAGAAATCAAGGAGCATT-3’
	Reverse	5’-TCACTCTTCACCTGCTCCAC-3’
iNOS	Forward	5’-CCCTTCCGAAGTTTCTGGCAGC-3’
	Reverse	5’-GGCTGTCAGAGCCTCGTGGCTTTGG-3’
MCP-1	Forward	5’-GAAGGAATGGGTCCAGACAT-3’
	Reverse	5’-ACGGGTCAACTTCACATTCA-3’
TLR3	Forward	5’-GCTCATTCTCCCTTGCTC-3’
	Reverse	5’-CCCGAAAACATCCTTCTCAA-3’
TLR6	Forward	5’-CTTAATAGTCGGAAGCATGACCCCG-3’
	Reverse	5’-AAGGTTGGACCTCTGGTGAGTTCTG-3’
TNFα	Forward	5’-ATGAGAAGTTCCCAAATGGC-3’
	Reverse	5’-CTCCACTTGGTGGTTTGCTA-3’

Online Table III. Serum glucose, cholesterol, and triglyceride levels in mice fed Western diet for 14 to 16 weeks.

	ApoE$^{-/-}$ (n=5)	ApoE$^{-/-}$/LysM-DKO (n=5	P Value
Glucose (mg/dL)	147.2±4.5	138.4±3.7	0.17
Total Cholesterol (mg/dL)	916.5±36.5	867.6±35.9	0.36
Triglycerides (mg/dL)	124.4±7.9	116.5±6.2	0.26

Online Table IV. Circulating immune cell levels from mice fed Western diet for 14 to 16 weeks.

	ApoE$^{-/-}$ (n=5)	ApoE$^{-/-}$/LysM-DKO (n=5)	P Value
White Blood Cells (K/μL)	5.965±1.837	9.592±3.548	0.09
Neutrophils (K/μL)	2.397±0.771	4.436±1.696	0.05
Lymphocytes (K/μL)	3.172±1.419	4.500±1.947	0.27
Monocytes (K/μL)	0.270±0.037	0.514±0.281	0.12
Eosinophils (K/μL)	0.090±0.091	0.100±0.048	0.85
Basophils (K/μL)	0.030±0.040	0.046±0.023	0.51

Online Table V. Circulating immune cell levels from AAV-PSCK9 injected mice fed Western diet for 10 weeks.

	WT-PCSK9 (n=8)	LysM-DKO-PCSK9 (n=8)	P Value
White Blood Cells (K/μL)	5.895±1.45	7.423±2.684	0.18
Neutrophils (K/μL)	1.923±0.412	2.488±0.964	0.16
Lymphocytes (K/μL)	3.599±1.146	4.376±1.640	0.29
Monocytes (K/μL)	0.274±0.113	0.333±0.188	0.46
Eosinophils (K/μL)	0.084±0.049	0.189±0.131	0.06
Basophils (K/μL)	0.014±0.009	0.038±0.039	0.14

Online Supplemental References:

1 Chen, H., Ko, G., Zatti, A., Di Giacomo, G., Liu, L., Raiteri, E., Perucco, E., Collesi, C., Min, W., Zeiss, C., De Camilli, P. & Cremona, O. Embryonic arrest at midgestation and disruption of Notch signaling produced by the absence of both epsin 1 and epsin 2 in mice. *Proc Natl Acad Sci U S A* **106**, 13838-13843, doi:10.1073/pnas.0907008106 (2009).

2 Pasula, S. *et al.* Endothelial epsin deficiency decreases tumor growth by enhancing VEGF signaling. *J Clin Invest* **122**, 4424-4438, doi:10.1172/JCI64537 (2012).

3 Bjorklund, M. M., Hollensen, A. K., Hagensen, M. K., Dagnaes-Hansen, F., Christoffersen, C., Mikkelsen, J. G. & Bentzon, J. F. Induction of atherosclerosis in mice and hamsters without germline genetic engineering. *Circ Res* **114**, 1684-1689, doi:10.1161/CIRCRESAHA.114.302937 (2014).

4 Lougheed, M., Zhang, H. F. & Steinbrecher, U. P. Oxidized low density lipoprotein is resistant to cathepsins and accumulates within macrophages. *J Biol Chem* **266**, 14519-14525 (1991).

5 Chen, H., Fre, S., Slepnev, V. I., Capua, M. R., Takei, K., Butler, M. H., Di Fiore, P. P. & De Camilli, P. Epsin is an EH-domain-binding protein implicated in clathrin-mediated endocytosis. *Nature* **394**, 793-797, doi:10.1038/29555 (1998).

6 Rosenthal, J. A., Chen, H., Slepnev, V. I., Pellegrini, L., Salcini, A. E., Di Fiore, P. P. & De Camilli, P. The epsins define a family of proteins that interact with components of the clathrin coat and contain a new protein module. *J Biol Chem* **274**, 33959-33965 (1999).

7 Tessneer, K. L., Pasula, S., Cai, X., Dong, Y., McManus, J., Liu, X., Yu, L., Hahn, S., Chang, B., Chen, Y., Griffin, C., Xia, L., Adams, R. H. & Chen, H. Genetic reduction of vascular endothelial growth factor receptor 2 rescues aberrant angiogenesis caused by epsin deficiency. *Arterioscler Thromb Vasc Biol* **34**, 331-337, doi:10.1161/ATVBAHA.113.302586 (2014).

8 Andres-Manzano, M. J., Andres, V. & Dorado, B. Oil Red O and Hematoxylin and Eosin Staining for Quantification of Atherosclerosis Burden in Mouse Aorta and Aortic Root. *Methods Mol Biol* **1339**, 85-99, doi:10.1007/978-1-4939-2929-0_5 (2015).

9 Mohanta, S., Yin, C., Weber, C., Hu, D. & Habenicht, A. J. Aorta Atherosclerosis Lesion Analysis in Hyperlipidemic Mice. *Bio Protoc* **6** (2016).

10 Venegas-Pino, D. E., Banko, N., Khan, M. I., Shi, Y. & Werstuck, G. H. Quantitative analysis and characterization of atherosclerotic lesions in the murine aortic sinus. *J Vis Exp*, 50933, doi:10.3791/50933 (2013).

11 Melo, R. C., D'Avila, H., Bozza, P. T. & Weller, P. F. Imaging lipid bodies within leukocytes with different light microscopy techniques. *Methods Mol Biol* **689**, 149-161, doi:10.1007/978-1-60761-950-5_9 (2011).

12 Tao, H., Yancey, P. G., Babaev, V. R., Blakemore, J. L., Zhang, Y., Ding, L., Fazio, S. & Linton, M. F. Macrophage SR-BI mediates efferocytosis via Src/PI3K/Rac1 signaling and reduces atherosclerotic lesion necrosis. *Journal of lipid research* **56**, 1449-1460, doi:10.1194/jlr.M056689 (2015).

13 Greenfield, E. A. Sampling and Preparation of Mouse and Rat Serum. *Cold Spring Harb Protoc* **2017**, pdb prot100271, doi:10.1101/pdb.prot100271 (2017).

14 Barski, O. A., Xie, Z., Baba, S. P., Sithu, S. D., Agarwal, A., Cai, J., Bhatnagar, A. & Srivastava, S. Dietary carnosine prevents early atherosclerotic lesion formation in apolipoprotein E-null mice. *Arterioscler Thromb Vasc Biol* **33**, 1162-1170, doi:10.1161/ATVBAHA.112.300572 (2013).

15 Sithu, S. D., Malovichko, M. V., Riggs, K. A., Wickramasinghe, N. S., Winner, M. G., Agarwal, A., Hamed-Berair, R. E., Kalani, A., Riggs, D. W., Bhatnagar, A. & Srivastava, S. Atherogenesis and metabolic dysregulation in LDL receptor-knockout rats. *JCI Insight* **2**, doi:10.1172/jci.insight.86442 (2017).
16 Srivastava, S., Vladykovskaya, E., Barski, O. A., Spite, M., Kaiserova, K., Petrash, J. M., Chung, S. S., Hunt, G., Dawn, B. & Bhatnagar, A. Aldose reductase protects against early atherosclerotic lesion formation in apolipoprotein E-null mice. *Circ Res* **105**, 793-802, doi:10.1161/CIRCRESAHA.109.200568 (2009).
17 Pal, R., Ke, Q., Pihan, G. A., Yesilaltay, A., Penman, M. L., Wang, L., Chitraju, C., Kang, P. M., Krieger, M. & Kocher, O. Carboxy-terminal deletion of the HDL receptor reduces receptor levels in liver and steroidogenic tissues, induces hypercholesterolemia, and causes fatal heart disease. *Am J Physiol Heart Circ Physiol* **311**, H1392-H1408, doi:10.1152/ajpheart.00463.2016 (2016).
18 Conklin, D. J. *et al.* Biomarkers of Chronic Acrolein Inhalation Exposure in Mice: Implications for Tobacco Product-Induced Toxicity. *Toxicol Sci* **158**, 263-274, doi:10.1093/toxsci/kfx095 (2017).
19 Malovichko, M. V., Zeller, I., Krivokhizhina, T. V., Xie, Z., Lorkiewicz, P., Agarwal, A., Wickramasinghe, N., Sithu, S. D., Shah, J., O'Toole, T., Rai, S. N., Bhatnagar, A., Conklin, D. J. & Srivastava, S. Systemic Toxicity of Smokeless Tobacco Products in Mice. *Nicotine Tob Res*, doi:10.1093/ntr/ntx230 (2017).
20 Prats, C., Gomez-Cabello, A., Nordby, P., Andersen, J. L., Helge, J. W., Dela, F., Baba, O. & Ploug, T. An optimized histochemical method to assess skeletal muscle glycogen and lipid stores reveals two metabolically distinct populations of type I muscle fibers. *PloS one* **8**, e77774, doi:10.1371/journal.pone.0077774 (2013).
21 Spangenburg, E. E., Pratt, S. J., Wohlers, L. M. & Lovering, R. M. Use of BODIPY (493/503) to visualize intramuscular lipid droplets in skeletal muscle. *J Biomed Biotechnol* **2011**, 598358, doi:10.1155/2011/598358 (2011).
22 Chang, B. *et al.* Epsin is required for Dishevelled stability and Wnt signalling activation in colon cancer development. *Nat Commun* **6**, 6380, doi:10.1038/ncomms7380 (2015).
23 Liu, X. *et al.* Temporal and spatial regulation of epsin abundance and VEGFR3 signaling are required for lymphatic valve formation and function. *Sci Signal* **7**, ra97, doi:10.1126/scisignal.2005413 (2014).
24 Rahman, H. N. *et al.* Selective Targeting of a Novel Epsin-VEGFR2 Interaction Promotes VEGF-Mediated Angiogenesis. *Circ Res* **118**, 957-969, doi:10.1161/CIRCRESAHA.115.307679 (2016).
25 Pineda-Torra, I., Gage, M., de Juan, A. & Pello, O. M. Isolation, Culture, and Polarization of Murine Bone Marrow-Derived and Peritoneal Macrophages. *Methods Mol Biol* **1339**, 101-109, doi:10.1007/978-1-4939-2929-0_6 (2015).
26 Chen, H. & De Camilli, P. The association of epsin with ubiquitinated cargo along the endocytic pathway is negatively regulated by its interaction with clathrin. *Proc Natl Acad Sci U S A* **102**, 2766-2771, doi:10.1073/pnas.0409719102 (2005).
27 Li, Y., Marzolo, M. P., van Kerkhof, P., Strous, G. J. & Bu, G. The YXXL motif, but not the two NPXY motifs, serves as the dominant endocytosis signal for low density lipoprotein receptor-related protein. *J Biol Chem* **275**, 17187-17194, doi:10.1074/jbc.M000490200 (2000).
28 Zilberberg, A., Yaniv, A. & Gazit, A. The low density lipoprotein receptor-1, LRP1, interacts with the human frizzled-1 (HFz1) and down-regulates the canonical Wnt signaling pathway. *J Biol Chem* **279**, 17535-17542, doi:10.1074/jbc.M311292200 (2004).
29 Jablonski, K. A., Amici, S. A., Webb, L. M., Ruiz-Rosado Jde, D., Popovich, P. G., Partida-Sanchez, S. & Guerau-de-Arellano, M. Novel Markers to Delineate Murine M1

and M2 Macrophages. *PloS one* **10**, e0145342, doi:10.1371/journal.pone.0145342 (2015).
30 Tatano, Y., Shimizu, T. & Tomioka, H. Unique macrophages different from M1/M2 macrophages inhibit T cell mitogenesis while upregulating Th17 polarization. *Sci Rep* **4**, 4146, doi:10.1038/srep04146 (2014).
31 Hoff, H. F., Gaubatz, J. W. & Gotto, A. M., Jr. Apo B concentration in the normal human aorta. *Biochem Biophys Res Commun* **85**, 1424-1430 (1978).
32 Smith, E. B. Transport, interactions and retention of plasma proteins in the intima: the barrier function of the internal elastic lamina. *Eur Heart J* **11 Suppl E**, 72-81 (1990).
33 Xu, S., Huang, Y., Xie, Y., Lan, T., Le, K., Chen, J., Chen, S., Gao, S., Xu, X., Shen, X., Huang, H. & Liu, P. Evaluation of foam cell formation in cultured macrophages: an improved method with Oil Red O staining and DiI-oxLDL uptake. *Cytotechnology* **62**, 473-481, doi:10.1007/s10616-010-9290-0 (2010).
34 Yancey, P. G., Blakemore, J., Ding, L., Fan, D., Overton, C. D., Zhang, Y., Linton, M. F. & Fazio, S. Macrophage LRP-1 controls plaque cellularity by regulating efferocytosis and Akt activation. *Arterioscler Thromb Vasc Biol* **30**, 787-795, doi:10.1161/ATVBAHA.109.202051 (2010).
35 Butcher, M. J., Herre, M., Ley, K. & Galkina, E. Flow cytometry analysis of immune cells within murine aortas. *J Vis Exp*, doi:10.3791/2848 (2011).
36 Galkina, E., Kadl, A., Sanders, J., Varughese, D., Sarembock, I. J. & Ley, K. Lymphocyte recruitment into the aortic wall before and during development of atherosclerosis is partially L-selectin dependent. *The Journal of experimental medicine* **203**, 1273-1282, doi:10.1084/jem.20052205 (2006).
37 Gjurich, B. N., Taghavie-Moghadam, P. L. & Galkina, E. V. Flow Cytometric Analysis of Immune Cells Within Murine Aorta. *Methods Mol Biol* **1339**, 161-175, doi:10.1007/978-1-4939-2929-0_11 (2015).
38 Cochain, C., Vafadarnejad, E., Arampatzi, P., Jaroslav, P., Winkels, H., Ley, K., Wolf, D., Saliba, A. E. & Zernecke, A. Single-Cell RNA-Seq Reveals the Transcriptional Landscape and Heterogeneity of Aortic Macrophages in Murine Atherosclerosis. *Circ Res*, doi:10.1161/CIRCRESAHA.117.312509 (2018).
39 Winkels, H. *et al.* Atlas of the Immune Cell Repertoire in Mouse Atherosclerosis Defined by Single-Cell RNA-Sequencing and Mass Cytometry. *Circ Res*, doi:10.1161/CIRCRESAHA.117.312513 (2018).
40 Yang, J., Zhang, L., Yu, C., Yang, X. F. & Wang, H. Monocyte and macrophage differentiation: circulation inflammatory monocyte as biomarker for inflammatory diseases. *Biomark Res* **2**, 1, doi:10.1186/2050-7771-2-1 (2014).
41 Mendez-David, I., El-Ali, Z., Hen, R., Falissard, B., Corruble, E., Gardier, A. M., Kerdine-Romer, S. & David, D. J. A method for biomarker measurements in peripheral blood mononuclear cells isolated from anxious and depressed mice: beta-arrestin 1 protein levels in depression and treatment. *Front Pharmacol* **4**, 124, doi:10.3389/fphar.2013.00124 (2013).
42 Chen, Z., Huang, A., Sun, J., Jiang, T., Qin, F. X. & Wu, A. Inference of immune cell composition on the expression profiles of mouse tissue. *Sci Rep* **7**, 40508, doi:10.1038/srep40508 (2017).
43 Swamydas, M. & Lionakis, M. S. Isolation, purification and labeling of mouse bone marrow neutrophils for functional studies and adoptive transfer experiments. *J Vis Exp*, e50586, doi:10.3791/50586 (2013).
44 Caplen, N. J., Parrish, S., Imani, F., Fire, A. & Morgan, R. A. Specific inhibition of gene expression by small double-stranded RNAs in invertebrate and vertebrate systems. *Proc Natl Acad Sci U S A* **98**, 9742-9747, doi:10.1073/pnas.171251798 (2001).

45 Scott, D. B., Michailidis, I., Mu, Y., Logothetis, D. & Ehlers, M. D. Endocytosis and degradative sorting of NMDA receptors by conserved membrane-proximal signals. *J Neurosci* **24**, 7096-7109, doi:10.1523/JNEUROSCI.0780-04.2004 (2004).

Online Figure I

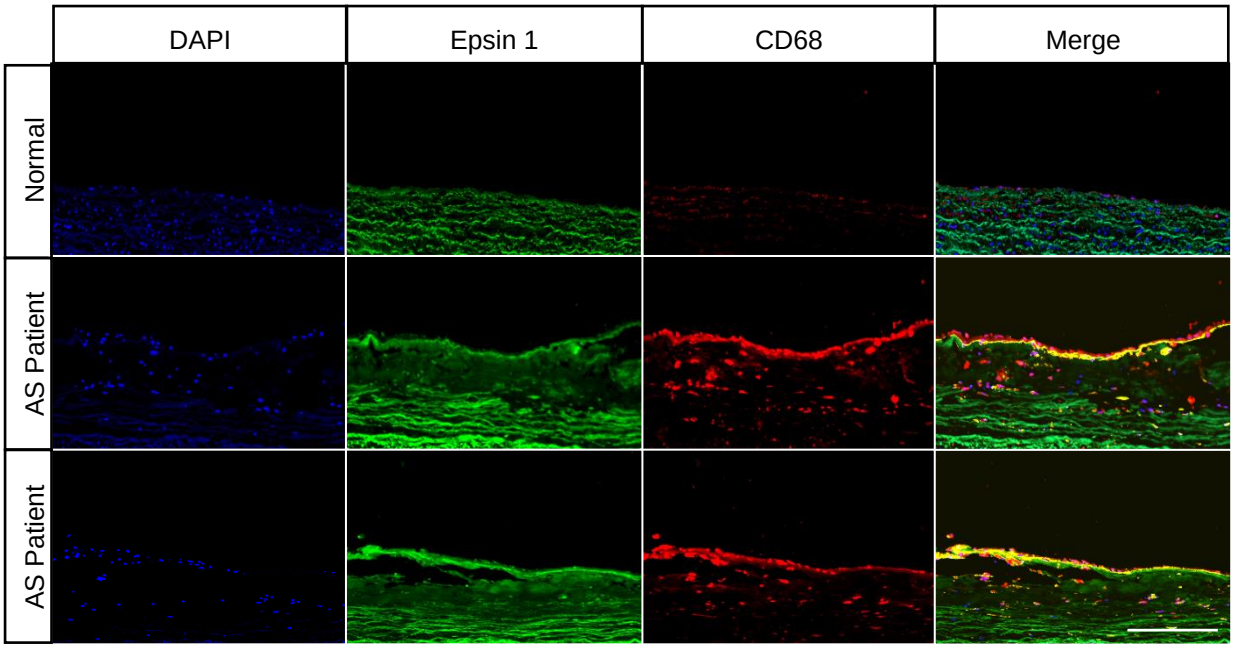

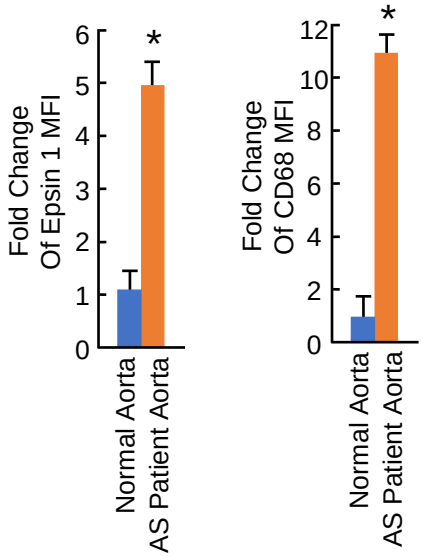

Online Figure II

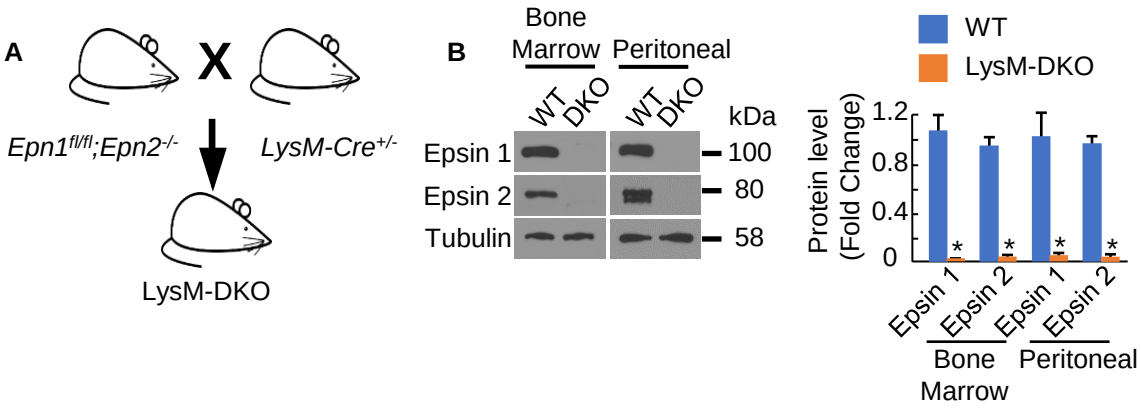

Online Figure III

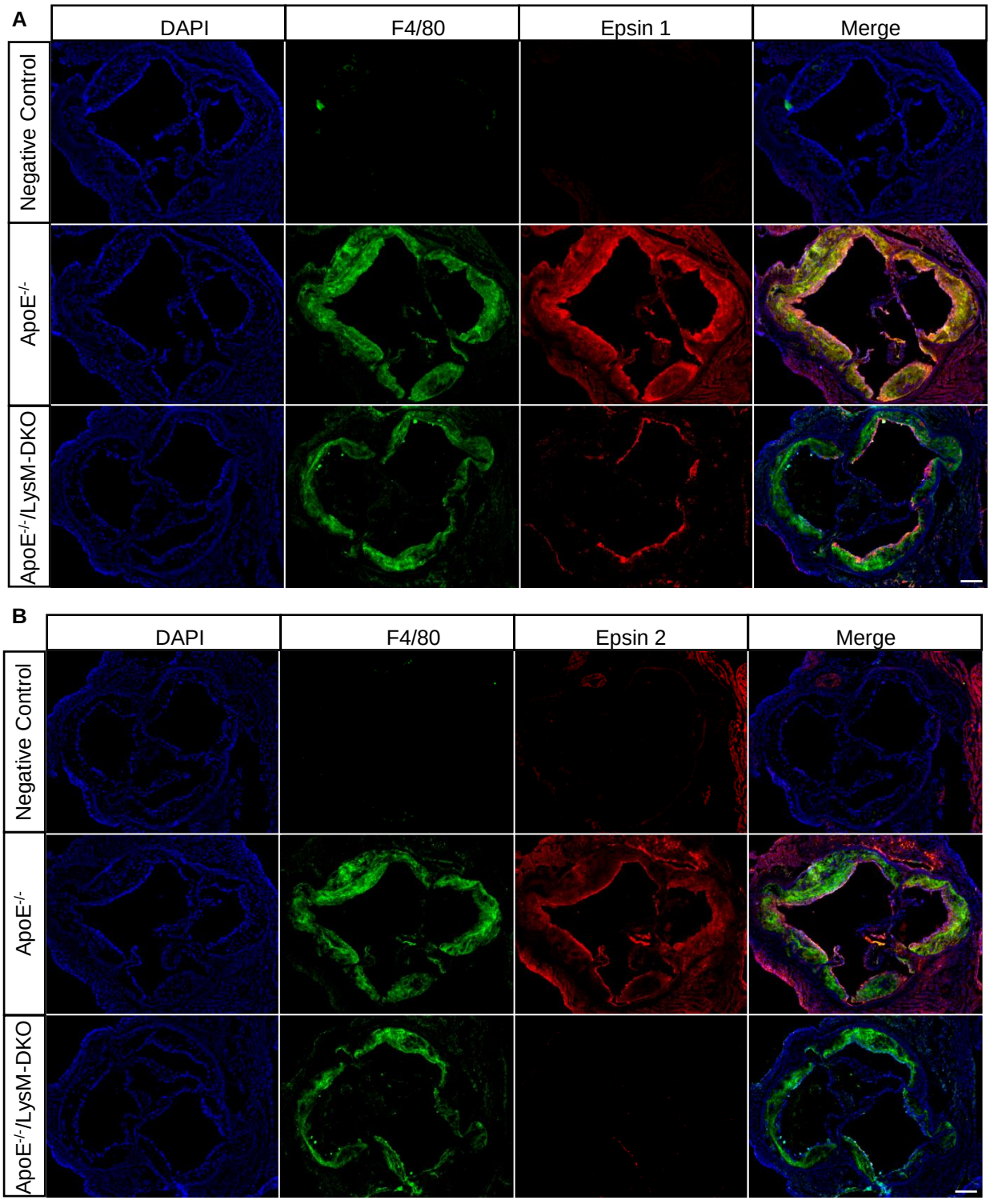

Online Figure IV

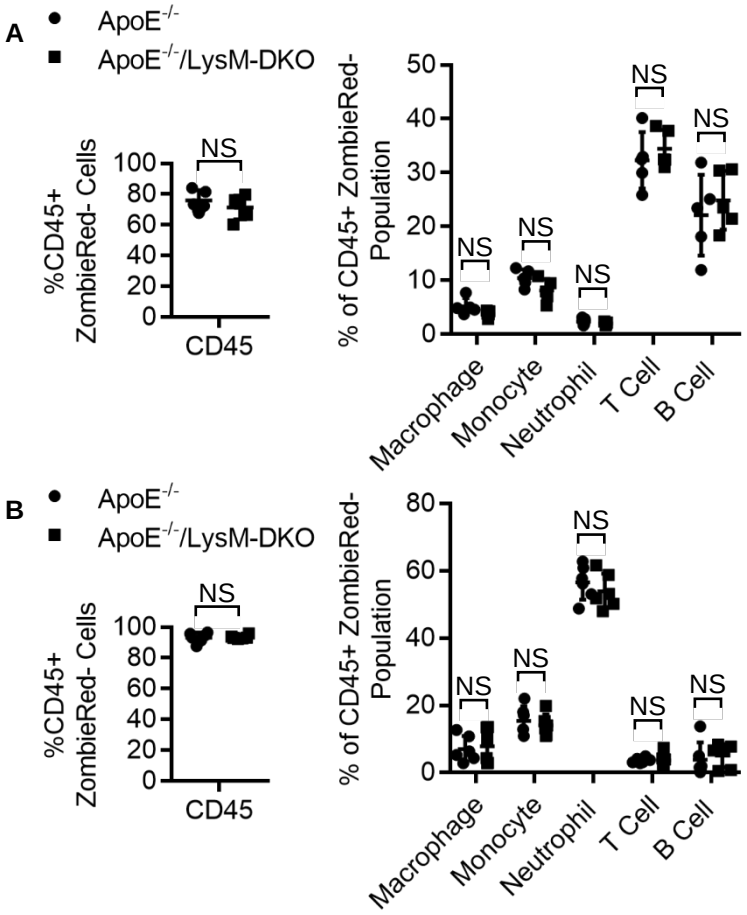

Online Figure V

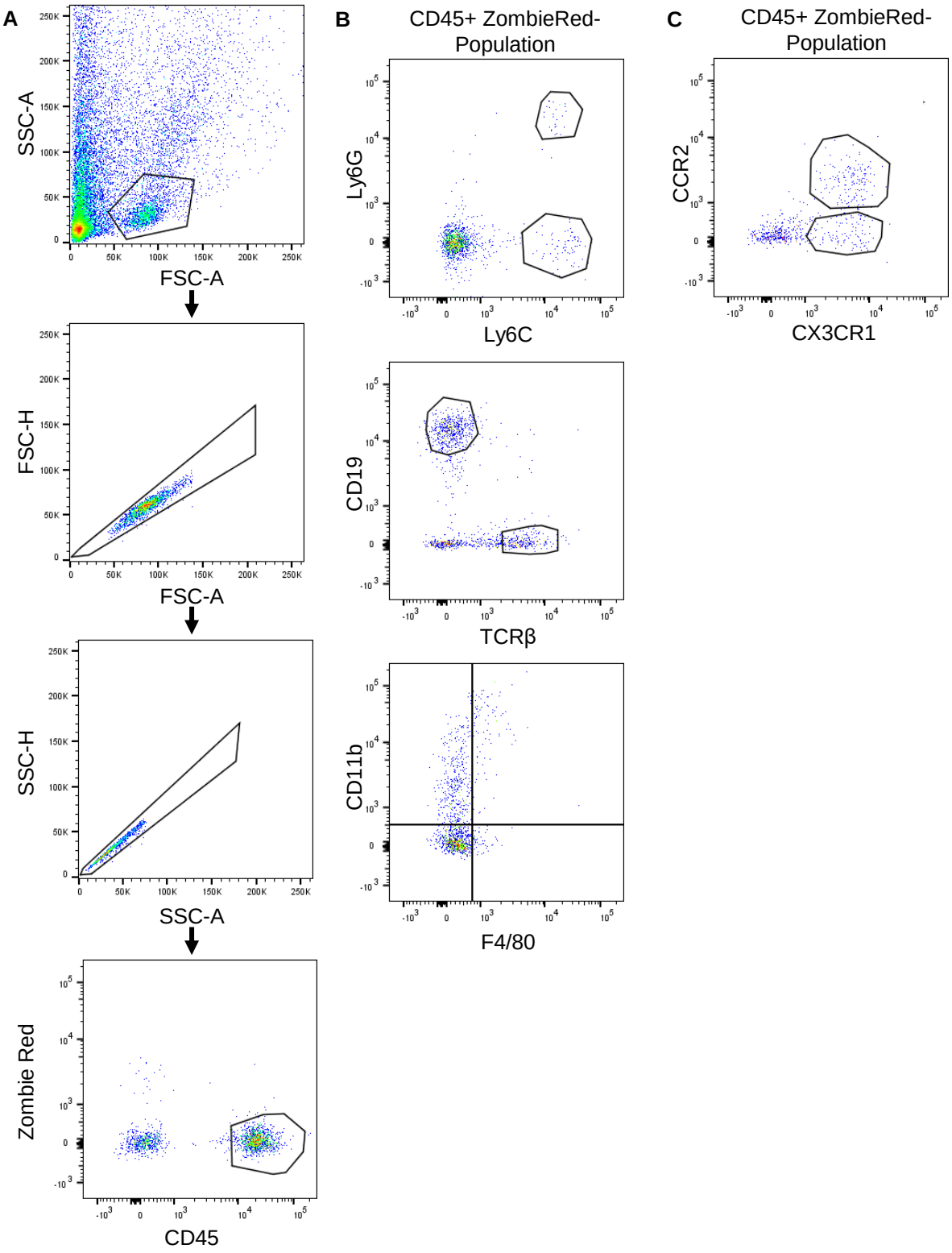

Online Figure VI

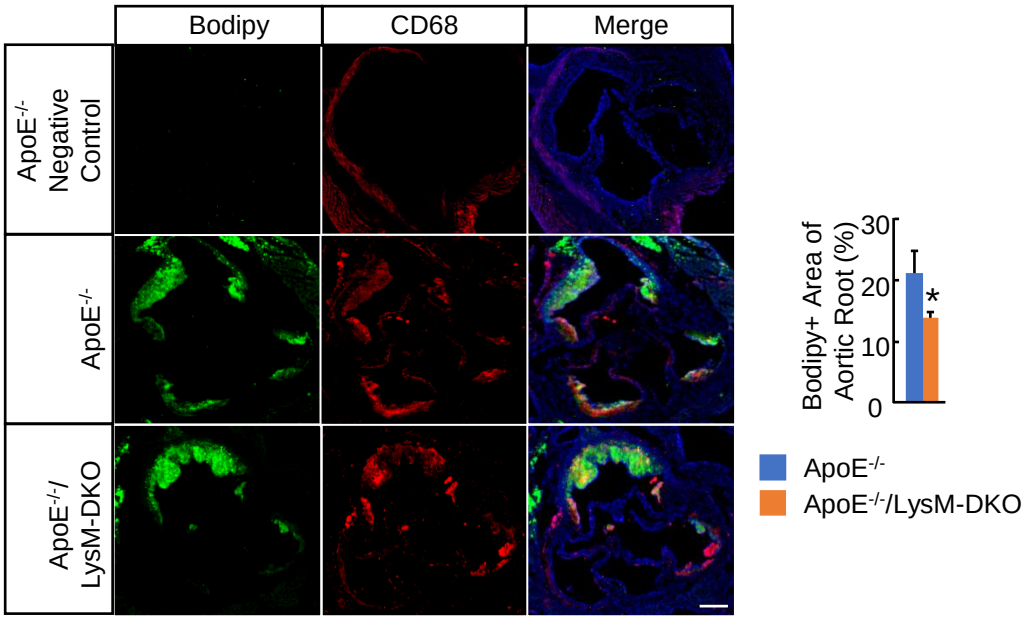

Online Figure VII

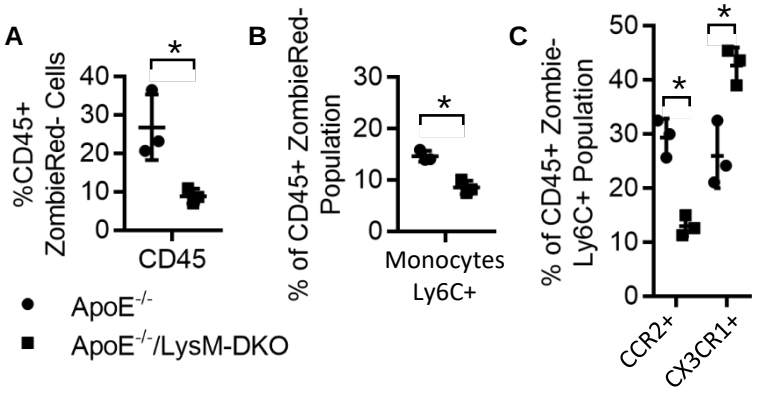

Online Figure VIII

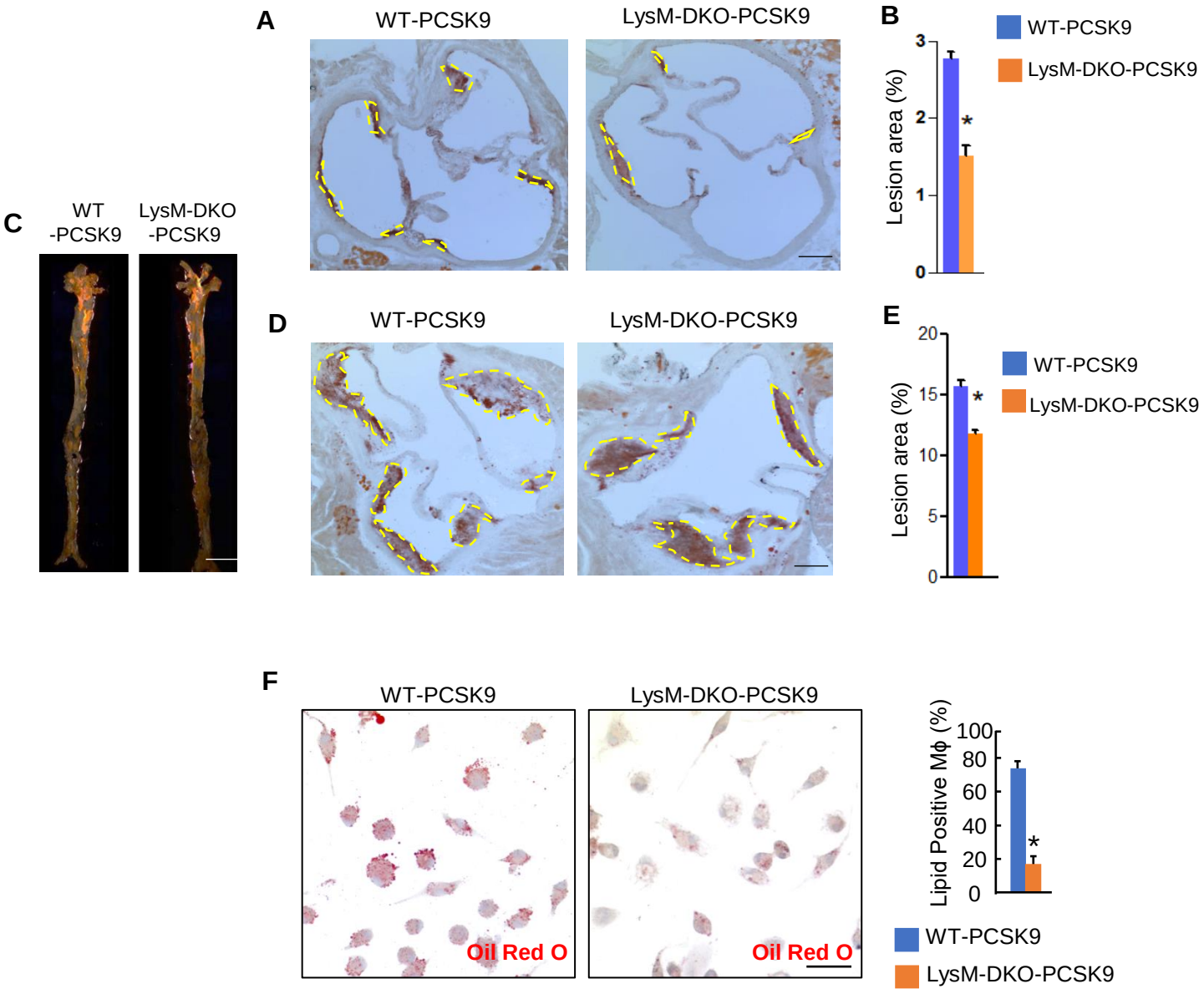

Online Figure IX

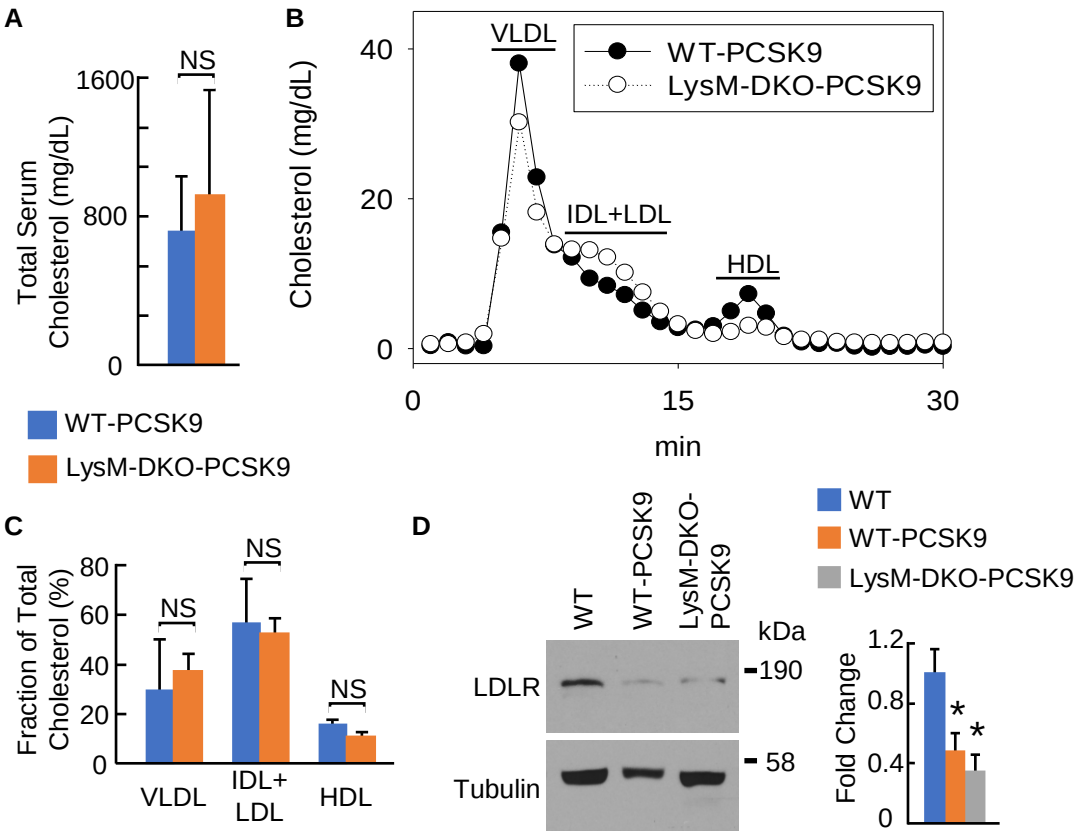

Online Figure X

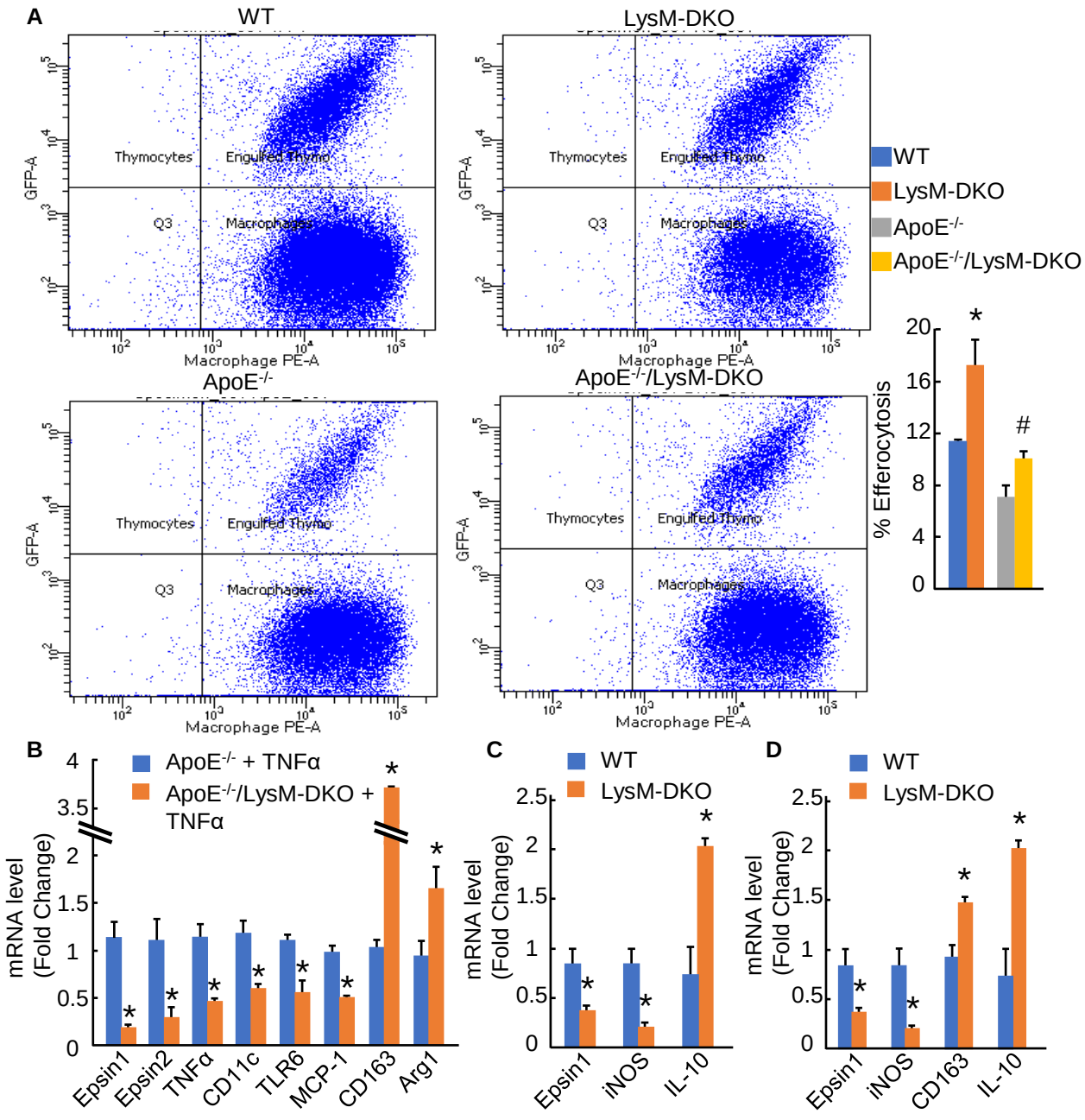

Online Figure XI

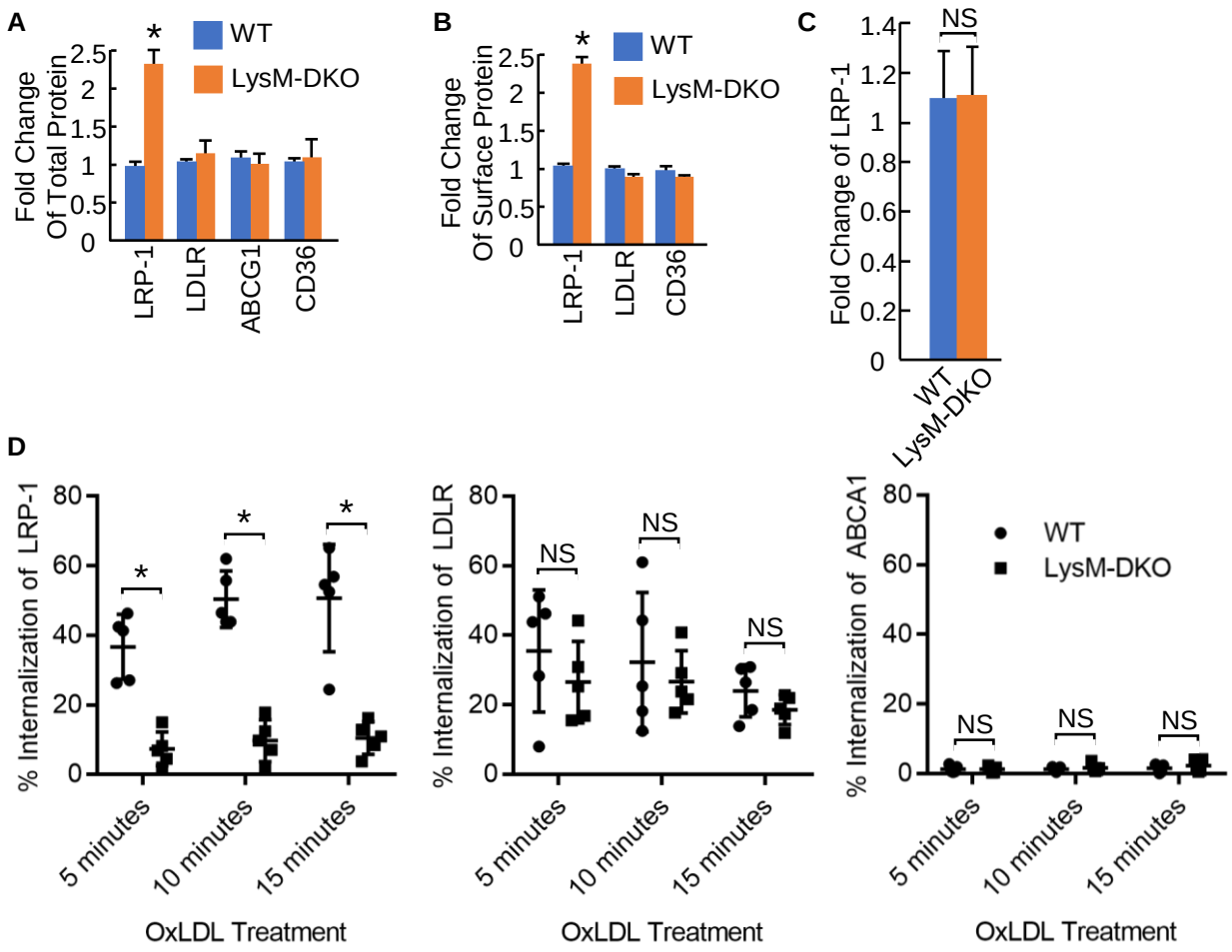

Online Figure XII

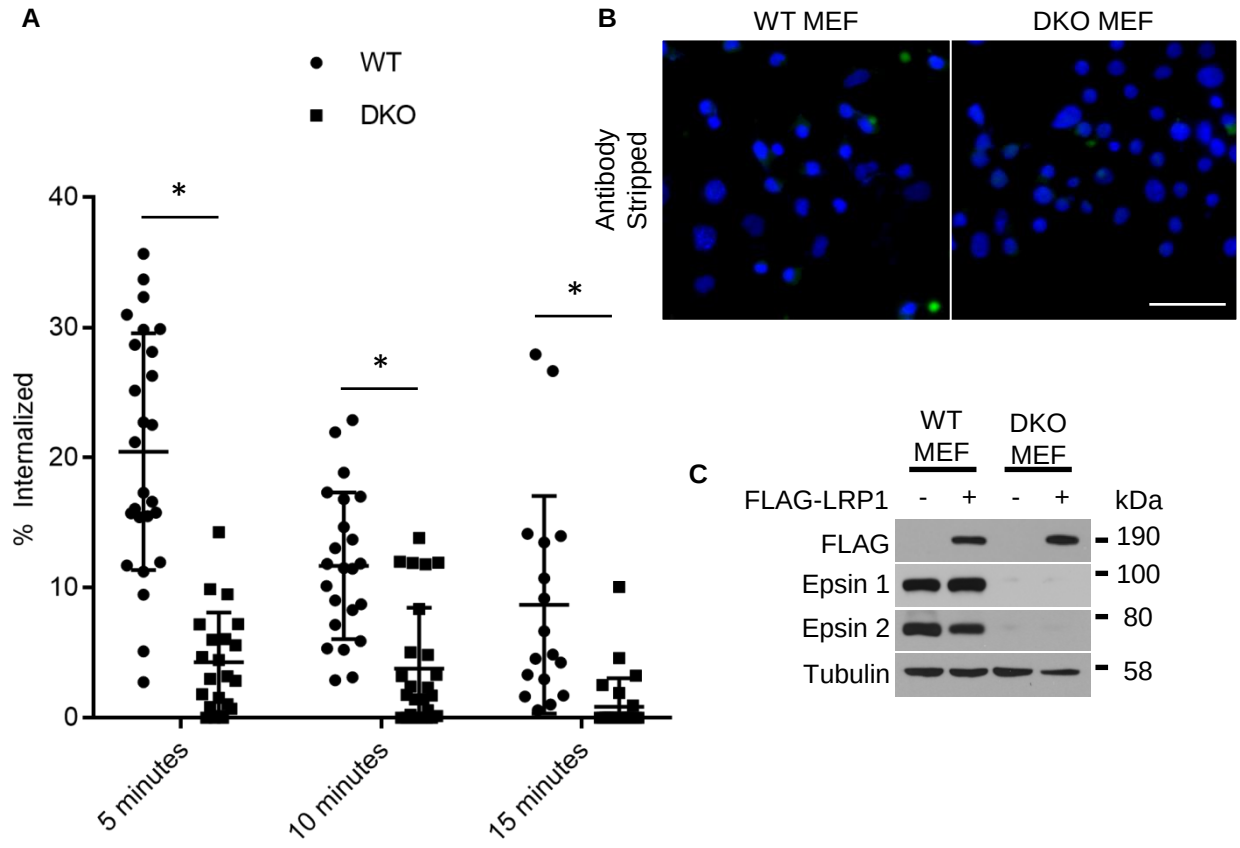

Online Figure XIII

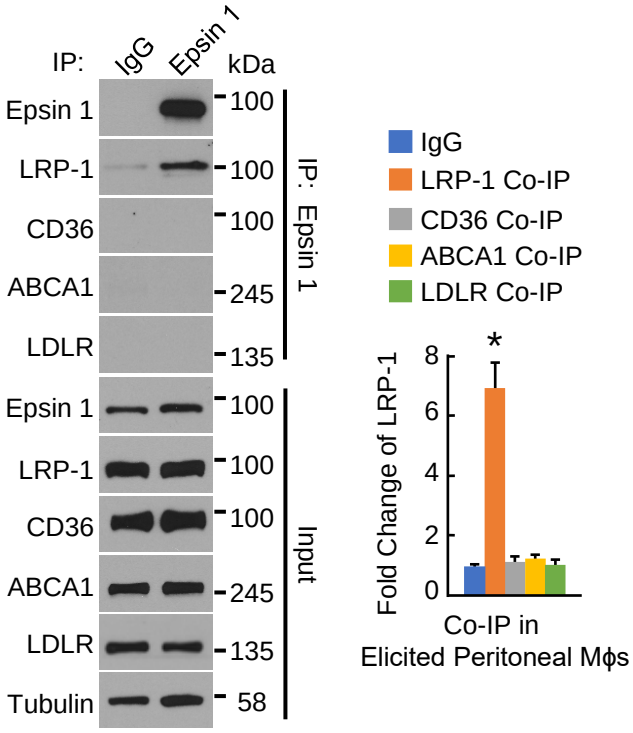

Online Figure XIV